

Crystal Structure Implies That Cyclophilin Predominantly Catalyzes the *Trans* to *Cis* Isomerization^{†,‡}

Yingdong Zhao and Hengming Ke*

Department of Biochemistry and Biophysics, School of Medicine, The University of North Carolina, Chapel Hill, North Carolina 27599

Received February 6, 1996; Revised Manuscript Received April 10, 1996[®]

ABSTRACT: The crystal structure of human recombinant cyclophilin A complexed with a substrate of succinyl-Ala-Ala-Pro-Phe-*p*-nitroanilide (AAPF) has been determined and refined to an *R*-factor of 0.189 at 2.4 Å resolution. The structure revealed only the *cis* form of the substrate bound to cyclophilin A in a stoichiometry of 1:1. This binding ratio is different from the structure of cyclophilin A complexed with the tetrapeptide *N*-acetyl-Ala-Ala-Pro-Ala-amidomethylcoumarin. Model docking revealed that the *trans* form of AAPF does not fit into the active site. The observation that only the *cis* form of AAPF binds to cyclophilin A implies that cyclophilin A predominantly catalyzes the *trans* to *cis* isomerization of a peptidyl-prolyl amide bond. On the basis of the structure, it is proposed that Arg55 hydrogen-bonds to the nitrogen to deconjugate the resonance of the prolyl amide bond and thus facilitates the *cis*–*trans* rotation.

As a receptor of the immunosuppressive drug cyclosporin A (CsA)¹ (Handschumacher et al., 1984), cyclophilin (CyP) complexed with CsA binds to and inhibits calcineurin (Liu et al., 1991; Haddy et al., 1992; Swanson, et al., 1992; Fruman et al., 1992), a serine/threonine phosphatase, and a Ca²⁺-dependent calmodulin binding protein (Klee et al., 1988). As an enzyme, cyclophilin catalyzes the isomerization of peptidyl-prolyl amide bonds (Fischer et al., 1989; Takahashi et al., 1989). The *cis*–*trans* isomerization has been considered to be involved in protein folding, as shown in *in vitro* experiments in which cyclophilin influenced the folding of several proteins: collagen or procollagen (Bächinger, 1987; Davis et al., 1989; Steinmann et al., 1991), chymotrypsin inhibitor 2 (Jackson & Fersht, 1991), carbonic anhydrase II (Fransson et al., 1992; Freskgård et al., 1992), and ribonuclease (Lang et al., 1987; Kiefhaber et al., 1990; Schönbrunner et al., 1991). On the other hand, the cyclophilin homolog *NinaA* forms a stable complex *in vivo* with rhodopsin (Baker et al., 1994), implying that cyclophilin may serve as a chaperone to transport proteins to a proper intracellular location. Similarly, cyclophilin 40 forms a chaperone complex with steroid receptor and heat shock proteins (Johnson & Toft, 1994). In addition, it was reported that incorporation of cyclophilin A is required for full infectious activity of human type 1 immunodeficiency virus (Franke et al., 1994; Thall et al., 1994).

A wealth of information on the three-dimensional structures is available for the unligated recombinant human T cell cyclophilin A (Ke et al., 1991; Ke, 1992), CyPA complexed with a proline-containing tetrapeptide (Kallen et al., 1991;

Kallen & Walkinshaw, 1992) and a dipeptide Ala-Pro (Ke et al., 1993a), CyPA complexed with CsA or its derivative (Pflügl et al., 1993; Thériault et al., 1993; Mikol et al., 1993; Ke et al., 1994), murine CyPC complexed with CsA (Ke et al., 1993b), and the human CyPB–CsA complex (Mikol et al., 1994). However, it is unknown whether CyP catalyzes the *cis*–*trans* isomerization with equal rates for both directions. We describe here the structure of CyPA complexed with succinyl-Ala-Ala-Pro-Phe-*p*-nitroanilide (AAPF) at 2.4 Å resolution. Since AAPF is a substrate commonly used for the assay of peptidyl-prolyl *cis*–*trans* isomerization of both cyclophilins and FK506 binding proteins (FKBP), the structure of CyPA–AAPF may provide insight into the mechanism of the catalysis.

METHODS

Recombinant human CyPA was purified as previously described (Liu et al., 1990). The tetrapeptide AAPF was purchased from BACHEM (catalog no. L1400). Cocrystals of the CyPA–AAPF complex were grown at room temperature by the vapor diffusion method. The well buffer was 100 mM Tris-HCl (pH 8.2), 46% saturated ammonium sulfate (AS), and 0.5 mM sodium azide. The protein drop contained 50 mM Tris-HCl (pH 8.2), 3% saturated AS, 0.2 mM sodium azide, 0.8 mM AAPF, 0.6 mM CyPA, 4% dimethyl sulfoxide, and 0.25% glycerol. The crystals were formed in 15–20 days with a typical size of 0.15 × 0.25 × 0.9 mm³. The space group is *P*2₁2₁2₁ with cell parameters of *a* = 37.8 Å, *b* = 109.2 Å, and *c* = 118.7 Å. Two molecules of the CyPA–AAPF complex exist in the crystallographic asymmetric unit. Diffraction data were collected on the Rigaku phosphate image plate system and were processed by the program DENZO (Table 1).

The structure was solved by the molecular replacement program AMoRe (Navaza, 1994) using the unligated CyPA as the initial model. The cross-rotation function of AMoRe revealed two peaks which have similar rotational orientations (Table 1). The final translational search for the two

[†] This work was supported by NIH Grant AI33072.

[‡] The atomic coordinates have been deposited in the Protein Data Bank, Chemistry Department, Brookhaven National Laboratory, Upton, NY 11973, with entry 1RMH.

* Corresponding author. Tel: (919)-966-2244. Fax: (919)-966-2852. email: hke@med.unc.edu.

[®] Abstract published in *Advance ACS Abstracts*, June 1, 1996.

¹ Abbreviations: CyP, cyclophilin; CyPA, cyclophilin A; CyPC, cyclophilin C; AAPF, succinyl-Ala-Ala-Pro-Phe-*p*-nitroanilide; CsA, cyclosporin A; FKBP, FK506 binding protein; AAPA-amc, *N*-acetyl-Ala-Ala-Pro-Ala-amidomethylcoumarin.

Table 1: Structure Determination of CyPA–AAPF

space group	$P2_12_12_1$
unit cell (Å)	$a = 37.8, b = 109.2, c = 118.7$
total measurements	50534
unique reflections	16668
resolution (Å)	2.4
overall completeness	88.7%
last shell completeness (2.40–2.51 Å)	73.1%
reflection ($I/\sigma > 2$)	16668 (100%)
R_{merge}	0.081
molecular replacement ^a	$\alpha = 135^\circ, \beta = 71^\circ, \gamma = 275^\circ,$ $T_x = 0.022, T_y = 0.538, T_z = 0.636$ $\alpha = 132^\circ, \beta = 80^\circ, \gamma = 284^\circ,$ $T_x = 0.089, T_y = 0.120, T_z = 0.166$
refinement	two CyPA (2516 atoms) and AAPF (90 atoms) + 38 waters, $R = 0.189$, $R_{\text{free}} = 0.252$ for 16110 reflections at 8.0–2.4 Å
RMS bond length deviations	0.013 Å
RMS bond angle deviations	3.1°

^a As defined in AmoRe (Navaza, 1994).

molecules resulted in a correlation coefficient of 0.767 and an R -factor of 0.286 for the data between 15 and 2.4 Å resolution. The molecular models were built by the program FRODO linked to the ESV10 graphic system (Jones, 1982) and refined by X-PLOR (Brünger et al., 1987) in a Decstation alpha computer. There is no restraint applied to the B refinement. The occupancy was not refined but fixed as 1 for all atoms of CyPA, the tetrapeptide, and solvent molecules. The *cis* prolyl peptide bond of AAPF was built by using the program FRODO and refined under a restraint of the *trans* peptide with a low force constant of 5 in comparison to 100 for other peptide bonds.

RESULTS AND DISCUSSION

Dimeric Structure of the CyPA–AAPF Complex. Two molecules of CyPA (residues 2–165, 2516 atoms) and AAPF (90 atoms) and 38 waters in the asymmetric unit were finally refined to an R -factor of 0.189 ($R_{\text{free}} = 0.252$) against 16 110 reflections which are stronger than $2I/\sigma$ at 8.0–2.4 Å resolution. The root-mean-squared errors from the ideal values were 0.013 Å and 3.1° for the bond length and bond angle, respectively. The electron density was excellent for most residues except for some side chains of the surface residues. The N-terminal residue was not included in the model because of lack of electron density. The structure has good molecular geometry, as revealed by a Ramachandran plot where all amino acids in the finally refined structure have backbone conformations located at the energy-favored regions (Ramachandran, 1968; data not shown). Two molecules of the CyPA–AAPF complex in the crystallographic asymmetric unit are related by a 2-fold axis which is very close to the crystallographic y axis (Figure 1). Superposition of the two monomers revealed positional displacements of 0.18 Å for C_α atoms and 0.35 Å for all atoms, indicating that the molecules in the asymmetric unit have very similar molecular conformations. The monomeric structure of the CyPA–AAPF complex is an eight-stranded β -barrel with a hydrophobic core at the center of the molecule, and the binding site of AAPF is located on the surface of the enzyme.

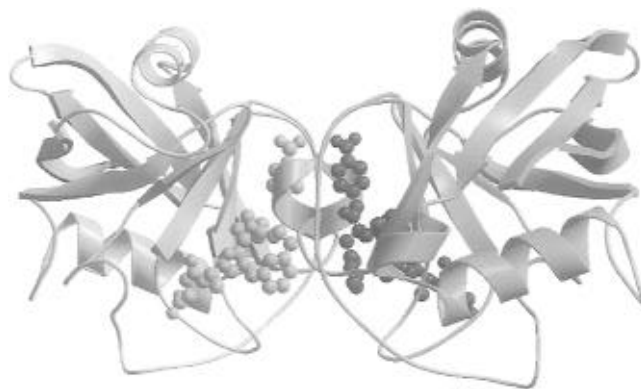


FIGURE 1: Ribbon diagram of dimeric CyPA–AAPF. AAPF (ball and stick) binds to the hydrophobic pocket in the surface of cyclophilin and contacts each other in the dimer. The molecular 2-fold axis is located in the vertical direction.

The *Cis* Form of AAPF Binds to CyPA. Each CyPA molecule binds one molecule of AAPF. Residues of CyPA involved in the interactions with AAPF include Arg55, Ile57, Phe60, Met61, Gln63, Ala101, Asn102, Gln111, Phe113, Trp121, Leu122, and His126 (Figure 2). Four hydrogen bonds, which are consistently observed in both molecules of the dimer in the crystallographic asymmetric unit, are formed between Ala2 N of AAPF and Asn102 O of CyPA, Pro3 O and Arg55 NH1, Pro3 O and Arg55 NH2, and Phe4 O and Trp121 NE1 (Table 2). In addition, the side chain of Arg148 of CyPA hydrogen-bonds to the nitro group of aniline of AAPF in molecule A, but the N–O distance for the same interaction in molecule B is 3.6 Å, much longer than a hydrogen bond. Since Arg148 is partially disordered as indicated by its weak electron density and high B -factor (average 63 Å² for the side chain), we are not sure whether this asymmetric interaction of Arg148 with AAPF is due to multiple conformations of Arg148 or due to an artifact resulting from the structure refinement. The succinyl group of AAPF forms two hydrogen bonds with two water molecules but does not directly interact with CyPA (Table 2). In addition to hydrogen bonding, AAPF forms numerous hydrophobic interactions with CyPA, most of which are associated with the C-terminal residues of Pro3, Phe4, and aniline of AAPF (Table 2).

Two AAPF molecules in the crystallographic asymmetric unit bind to CyPA in a very similar conformation (Table 3). Although all prolyl peptide bonds in the structure were restrained as a *trans* conformation with a small force constant of 5 during refinement, the torsional angles around the peptidyl-prolyl amide bonds of AAPF were refined to 14° and 21°, respectively, for the two molecules in the asymmetric unit, clearly defining the *cis* conformation of the substrate bound to CyPA. In contrast, the six proline residues of CyPA were refined to a *trans* conformation with an averaged deviation of 6.9°. The electron density was excellent for most atoms of the tetrapeptide (Figure 3) but slightly weaker for the succinyl group, perhaps due to lack of hydrogen bonding to CyP. The overall average B -factor of AAPF was refined to 32.6 Å² under fixed full occupancy, in comparison to 19.8 Å² for all the atoms in the protein molecule. However, the succinyl group, Ala1, and the side chain of Phe4 of the tetrapeptide had B -factors as high as 60 Å². If those atoms are excluded, the average B -factor for AAPF will be reduced to 21.5 Å². This value is quite comparable with the overall average B -factor of 19.8 Å² of

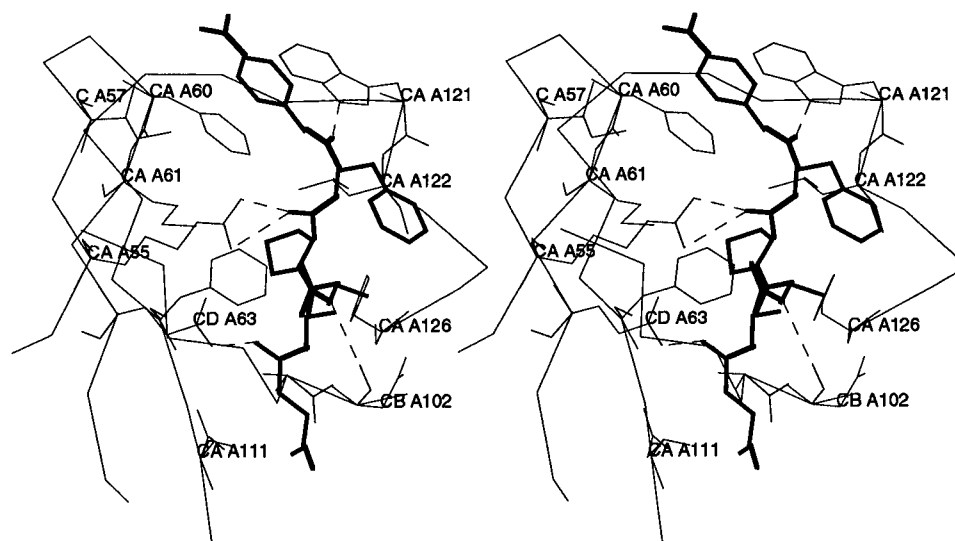


FIGURE 2: Stereo plot of the AAPF binding at the active site of CyPA. The thinner lines represent backbone traces and binding residues of CyPA. The thicker lines are AAPF. Hydrogen bonds (dotted lines) are formed between the side chain of Arg55 of CyPA and CO of Pro3 of AAPF, NE1 of Trp121 and CO of Phe4, and CO of Asn102 and N of Ala2. The side chain of Pro3 is located in a hydrophobic pocket made up of side chains of Phe60, Met61, Phe113, Leu122, and His126.

Table 2: Interactions between AAPF and CyPA

AAPF ^a	CyPA	distance (Å) ^b
Hydrogen Bonds		
Suc:OD1	Wat9	3.00 (A)
	Wat26	3.12 (A)
	Wat2	2.78 (B)
	Wat17	2.92 (B)
Suc:O	Wat19	2.91 (A)
Suc:O	Gln63:NE2	2.73 (A), 2.88 (B)
Ala2:N	Asn102:O	3.25 (A), 2.92 (B)
Pro3:O	Arg55:NH1	2.66 (A), 2.63 (B)
	Arg55:NH2	3.17 (A), 3.06 (B)
Phe4:O	Trp121:NE1	2.98 (A), 2.96 (B)
NA:OD1	Arg148:NH1	2.67 (A)
	Arg148:NH2	2.78 (A)
Hydrophobic or Polar Interactions		
Suc	Gln63 (A, B), Ash102 (A, B), Gln113 (A, B)	
Ala1	Arg55 (A, B), Asn102 (A)	
Ala2	Ala101 (A, B), Asn102 (A, B), His126 (A, B)	
Pro3	Arg55 (A, B), Phe60 (A, B), Met61 (A), Phe113 (A, B), Leu122 (A, B), His126 (A, B)	
Phe4	Trp121 (A, B)	
NA	Ile57 (A, B), Phe60 (A), Trp121 (A, B), Arg148 (A)	

^a Suc = succinyl; NA = nitroanilide. ^b A distance of 3.2–4.0 Å is defined as hydrophobic or polar interactions. The letters in parentheses represent interactions existing in molecule A or B.

the protein. The normal *B*-factor and excellent electron density indicate full occupancy and a single *cis* conformation of AAPF in the active site of CyPA, in spite of the fact that the low concentration of AAPF (0.8 mM) was used under the crystallization condition and that loose binding of AAPF to CyPA was reported (K_m value of about 1 mM) (Kofron et al., 1991).

The crystal structure of human recombinant CyPA complexed with *N*-acetyl-Ala-Ala-Pro-Ala-amidomethylcoumarin (AAPA-amc) (Kallen et al., 1991; Kallen & Walkinshaw, 1992) showed two coumarins and one N-terminus of the tetrapeptide bound to each molecule of CyPA. The *B*-factors for AAPA-amc ranged from 40 to 60 Å², implying partial occupancy of these sites (Kallen & Walkinshaw, 1992). These data could be interpreted either as two molecules of the tetrapeptide AAPA-amc or as one tetrapeptide linked with two conformations of the coumarin groups per active site,

in contrast to the binding stoichiometric ratio of 1:1 in our structure of the CyPA–AAPF complex. Since AAPF is the most commonly used substrate in assay of *cis*–*trans* isomerase of both cyclophilin and FK506 binding protein, we believe that one substrate per active site as revealed in our CyPA–AAPF structure should represent a normal binding stoichiometry for *cis*–*trans* isomerization by CyP while binding of two tetrapeptides per active site might be a special contribution of the coumarin group. Nevertheless, the CyPA–AAPA-amc structure showed the *cis* prolyl amide bond of the tetrapeptide bound to CyPA, consistent with the crystal structures of CyPA–Ala-Pro and CyPA–AAPF.

Ligation Does Not Change the Overall Structure of CyP. Crystal structures of the unligated CyPA, CyPA–Ala-Pro, CyPA–CsA, and CyPC–CsA were compared with CyPA–AAPF by superposition. The averaged displacements between these structures were 0.24–0.44 Å for C_α atoms and 0.50–0.70 Å for all atoms, indicating no substantial changes in the overall structure of CyP when ligands bind. However, small but significant changes were observed for some residues near the binding pocket. For example, C_α of Gly104 was displaced by about 1 Å, more than 3 times the average shift of 0.29 Å when AAPF binds to CyPA (Figure 4). In addition, residues 140–154 and regions around 69 and 81 had C_α displacements about 2 times the average value (Figure 4). These positional shifts appear to be necessary for the best fit of AAPF to the active site of CyPA, because these residues are nearby or close to the active site. In summary, the superposition revealed that CyP is rather rigid and its molecular conformation may change slightly to accommodate special requirements of ligands.

Can a Peptide with a Trans Prolyl Amide Bond Fit in the Active Site? All known crystal structures so far showed only the *cis* form of proline-containing peptides bound to CyP. However, NMR studies of the bound conformation of AAPF appear to be controversial. The transferred nuclear Overhauser effect (TRNOE) measurements by two-dimensional ¹H NMR in solution revealed a *cis*-like conformation of AAPF with the prolyl amide bond no more than 40° out of planarity (Kakalis & Armitage, 1994). In contrast, the one-

Table 3: Torsional Angles of AAPF^a

residue	ϕ	ψ	ω	χ_1	χ_2
Ala1	-82.0 (-77, -87)	-38.0 (-37, -39)	179.5 (180, 179)		
Ala2	-88.0 (-85, -91)	147.5 (147, 148)	17.5 (14, 21)		
Pro3	-81.0 (-78, -88)	146.0 (148, 144)	180.0 (177, -177)	37.0 (33, 41)	-43.5 (-44, -43)
Phe4	-92.5 (-91, -94)	129.0 (128, 130)	-175.5 (-177, -174)	-88.0 (-89, -87)	-47.0 (-48, -46)

^a The torsional angles are listed as an average value in the dimer in degrees, and the values in parentheses are angles for molecules 1 and 2.

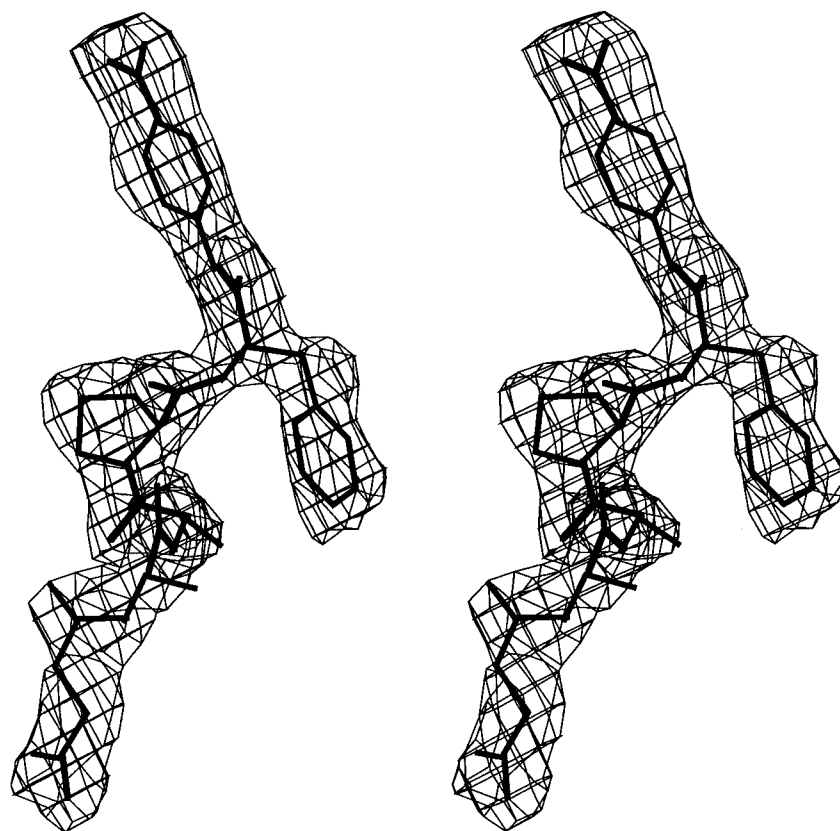


FIGURE 3: Stereo plot of the electron density for AAPF. The $(2F_o - F_c)$ map was calculated from the CyPA–AAPF structure in which AAPF was omitted. The density is contoured at 1σ . AAPF (thicker lines) fits the density very well, but the N-terminal succinyl and Ala1 and the side chain of Phe4 have B -factors ranging from 40 to 60 Å².

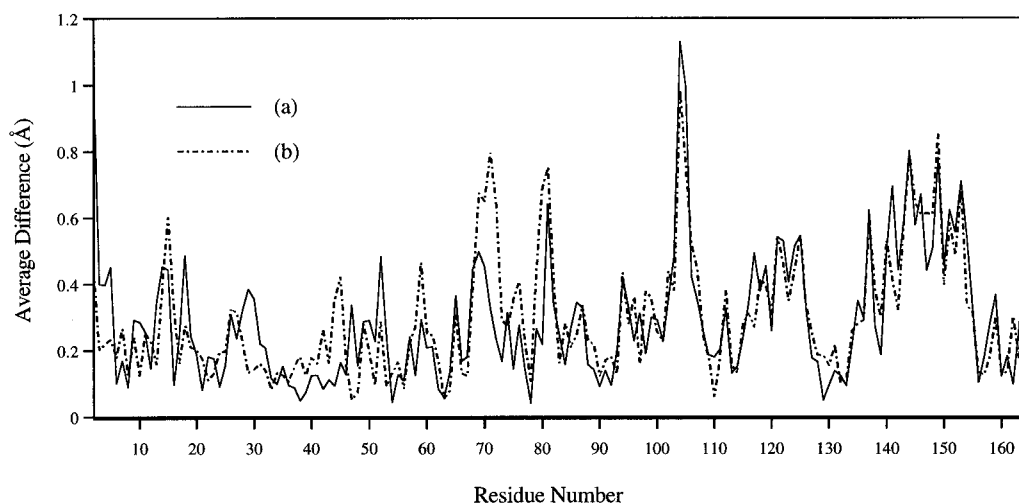


FIGURE 4: Plot of positional displacement of C_α atoms versus residues between the structures of unligated CyPA and CyPA–AAPF. The differences are presented by solid lines for molecule A and dotted lines for molecule B of CyPA–AAPF in the crystallographic asymmetric unit. The average displacement is 0.29 Å for the C_α atoms.

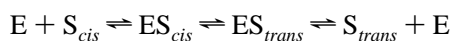
dimensional dynamic ¹H NMR spectroscopy in combination with protease-coupled PPIase assay suggested an equilibrium of 41% *trans* and 59% *cis* for the bound AAPF (Kern et al., 1995).

In order to explore whether the *trans* form can bind to the active site of CyPA, model-building was performed using the CyPA–AAPF structure. We assumed no changes in the overall structure of CyPA as a result of the above structure

superposition. The *trans* form of AAPF was generated by rotating the peptidyl-prolyl bond, while retaining the conformations of other bonds of AAPF as in the crystal structure. Two attempts were made to dock the *trans* form of the peptides into the active sites. Fixing the N-terminus of the ligand in the crystal structure and rotating the C-terminus placed peptides totally outside the binding pocket. Fixing the C-terminus and rotating the N-terminus docked peptides into the binding pocket better but still did not fit the *trans*-AAPF completely into the active site. In the second attempt at docking, the nitrogen of Ala2 of AAPF was too close (about 1.6 Å) to the backbone nitrogen of Asn102, and Ala1 of AAPF collapsed with the carbonyl of Asn102. For an entire fit of the *trans* AAPF, Asn102 has to be moved away by at least 3 Å. To accomplish this, three strands of residues 100–105, 106–109, and 81–85 of CyPA need to be shifted simultaneously because they interact with one another closely. This massive movement of several fragments seems unlikely to occur, because structure comparison has already revealed the rigidity of the CyPA molecule. Although the fit of the *trans* peptide was not exhaustively explored for other conformations, the result from model docking, that the *trans* form of substrate does not fit the active site, is consistent with the fact that the *trans* form of the peptide was not observed experimentally in the crystal structures.

In general, one may expect that both the substrate and the product of a reaction should bind to an enzyme although the binding strength may be substantially different. In contrast with most enzymatic reactions involving formation or breakage of a covalent bond, *cis*–*trans* isomerization generates two conformers which have identical chemical composition but different molecular structures. Thus, it needs to be understood whether and how both *cis* and *trans* forms of a substrate bind to the same pocket. Experimentally, all crystal structures revealed the unique binding of the *cis* form of the peptides Ala-Pro, AAPF, and AAPA-amc to CyP. These results may be interpreted as indicating either that the *trans* prolyl peptides are quickly converted to the *cis* form upon binding or that a portion of the *trans* form such as the C-terminus binds to CyP first and then CyP converts it to *cis* before binding the entire molecule.

CyP Predominantly Catalyzes the Trans to Cis Isomerization. The binding of AAPF in the crystal structure presumably represents an equilibrium state of the *cis* and *trans* forms of prolyl peptides bound to CyP, because diffraction data were collected in about 15 h, which should be long enough for a reaction with $k_{\text{cat}} = 1.3 \times 10^4 \text{ s}^{-1}$ to reach equilibrium (Kofron et al., 1991). It seems reasonable to assume the following pathway for *cis*–*trans* isomerization catalyzed by CyP (Kern et al., 1995):



where E = enzyme, S = substrate, and ES = the enzyme-substrate complex. By assuming that an enzyme cannot alter the equilibrium constant between the free and solution concentrations of substrate and product, Haldane (1930) showed that k_{cat}/K_m for the forward reaction over k_{cat}/K_m for the backward reaction equals K_{eq} , where $K_{\text{eq}} = [\text{product}]/[\text{substrate}]$. In the case of CyP, if K_{eq} is treated as unity (the observed $[\text{trans}]/[\text{cis}]$ ranges from 0.25 to 3 for proline-containing peptides; Grathwohl & Wüthrich, 1981), then k_{cat}/K_m for *trans* is equal to k_{cat}/K_m for *cis*. The absence of bound

trans AAPF in the crystal structure implies that the apparent dissociation constant K_m for *trans* is very large. Therefore, k_{cat} for the reaction of *trans* to *cis* must be much larger than k_{cat} for the reverse reaction.

Mechanism of the Cis–Trans Isomerization. Several mechanisms have been proposed for the *cis*–*trans* isomerization (Stein, 1993). In the covalent tetrahedral intermediate mechanism (Fischer et al., 1989), a cysteine or a nucleophilic residue was assumed to form a covalent bond with the carbonyl carbon as the intermediate. However, site-directed mutagenesis (Liu et al., 1990) and the X-ray structures (Ke, 1992) revealed no candidate nucleophile near the amide bond. Therefore, the carbon tetrahedral intermediate mechanism could probably be ruled out (Ke et al., 1993a).

A second mechanism is called “catalysis by distortion”, in which the N–C=O plane is distorted by binding to CyP and the intermediate is stabilized by the interaction with CyP (Harrison & Stein, 1990a). This mechanism is supported by the kinetic isotope effect, but no chemical groups which stabilize the intermediate were proposed.

A third mechanism assumes that the side chains of serine, threonine, or tyrosine protonate or hydrogen-bond to the imide nitrogen to deconjugate the O=C–N amide bond. Molecular orbital calculations indeed revealed that protonation on the nitrogen lowers the barrier for the *cis*–*trans* rotation (Kofron et al., 1991).

A fourth mechanism of “catalysis by desolvation” is based on the observation that the rate of *cis*–*trans* isomerization was significantly accelerated in nonpolar solvents (Wolfenden & Radzicka, 1991; Radzicka et al., 1992). The hydrophobic character of the active site supports this possibility.

Last, a solvent-assisted mechanism was proposed on the basis of the CyPA–Ala-Pro structure (Ke et al., 1993a). This mechanism assumes two steps of catalysis: desolvation by binding to the hydrophobic pocket and stabilization of the intermediate by a solvent molecule.

In general, the C–N amide bond is conjugated with the carbonyl group C=O to form a planar configuration of the amide bond. This conjugation gives the C–N bond a double bond character, and thus *cis*–*trans* isomerization of the prolyl amide bond needs to overcome the barrier to rotation. Any factors which can weaken the double bond character of the C–N amide bond are expected to accelerate the isomerization.

In the structure of CyPA complexed with the tetrapeptide AAPF, NH1 of the guanidine group of Arg55 forms a hydrogen bond with the carbonyl oxygen of proline of AAPF, while the NH2 atom is about 3.8 Å away from the nitrogen of proline of AAPF (Figure 2 and Table 2). These distances and the interactions in the crystal structure represent the ground state. However, this distance may be close enough for the guanidine nitrogen of Arg55 to approach the nitrogen of the amide bond so as to form a hydrogen bond with the lone pair electrons of the peptide nitrogen during catalysis [a diagram on this mechanism is shown in the accompanying paper by Zhao and Ke (1996)]. As a result, the double bond character of the amide bond might be substantially weakened, and the *cis*–*trans* isomerization is facilitated. This assumption is consistent with the observation that mutation of Arg55 to alanine retains less than 1% of the wild-type catalytic activity (Zydowsky et al., 1992). The crystal structure of CyPA–AAPF supports the mechanism of the “protonation on nitrogen” (Kofron et al., 1991) but pinpoints the catalytic

group as Arg55 instead of serine or tyrosine. The above mechanism involving a general acid catalysis of *cis*–*trans* isomerization by Arg55 is not in conflict with the observed pH independence of the *cis*–*trans* activity (Harrison & Stein, 1990b), since the guanidine group of Arg55 is expected to remain protonated at a pH range of 5.5–9.0.

In addition, the crystal structure of CyPA–AAPF revealed that the water molecule which was assumed to assist the *cis*–*trans* isomerization (Ke et al., 1993a) is spatially displaced by the N-terminus of AAPF. Therefore, the solvent-assisted mechanism for the *cis*–*trans* isomerization is not verified by the crystal structure of CyPA–AAPF. Two possible interpretations to this inconsistency, that (1) the dipeptides are not substrates but competitive inhibitors of CyP or (2) the tetrapeptides and dipeptides have different catalytic pathways, are discussed elsewhere (Zhao & Ke, 1996).

ACKNOWLEDGMENT

We thank Dr. R. Wolfenden for his critiques on the manuscript and discussion on *cis*–*trans* isomerization.

REFERENCES

- Bächinger, H. P. (1987) *J. Biol. Chem.* 262, 17144–17148.
- Baker, E. K., Colley, N. J., & Zuker, C. S. (1994) *EMBO J.* 13, 4886–4895.
- Brünger, A. T., Kuriyan, J., & Karplus, M. (1987) *Science* 235, 458–460.
- Davis, J. M., Boswell, B. A., & Bächinger, H. P. (1989) *J. Biol. Chem.* 264, 8956–8962.
- Fischer, G., Wittmann-Liebold, B., Lang, K., Kiefhaber, T., & Schmid, F. X. (1989) *Nature* 337, 476–478.
- Franke, E. K., Yuan, H. E. H., & Luban, J. (1994) *Nature* 372, 359–362.
- Fransson, C., Freskgård, P., Herbertsson, H., Johansson, Å., Jonasson, P., Mørtensson, L., Svensson, M., Jonsson, B., & Carlsson, U. (1992) *FEBS Lett.* 296, 90–94.
- Freskgård, P., Bergenhem, N., Jonsson, B., Svensson, M., & Carlsson, U. (1992) *Science* 258, 466–468.
- Fruman, D. A., Klee, C. B., Bierer, B. E., & Burakoff, S. J. (1992) *Proc. Natl. Acad. Sci. U.S.A.* 89, 3686–3690.
- Grathwohl, C., & Wüthrich, K. (1981) *Biopolymers* 20, 2623–2633.
- Haddy, A., Swanson, S. K. H., Born, T. L., & Rusnak, F. (1992) *FEBS Lett.* 314, 37–40.
- Haldane, J. B. S. (1930) *Enzyme*, Longmans,
- Handschumacher, R. E., Harding, M. W., Rice, J., & Drugge, R. J. (1984) *Science* 226, 544–547.
- Harrison, R. K., & Stein, R. L. (1990a) *Biochemistry* 29, 1684–1689.
- Harrison, R. K., & Stein, R. L. (1990b) *Biochemistry* 29, 3813–3816.
- Jackson, S. E., & Fersht, A. R. (1991) *Biochemistry* 30, 10436–10443.
- Johnson, J. L., & Toft, D. O. (1994) *J. Biol. Chem.* 269, 24989–24993.
- Jones, T. A. (1982) in *Computational crystallography* (Sayre, D., Ed.), pp 303–317, Oxford, London.
- Kakalis, L. T., & Armitage, I. M. (1994) *Biochemistry* 33, 1495–1501.
- Kallen, J., & Walkinshaw, M. D. (1992) *FEBS Lett.* 300, 286–290.
- Kallen, J., Spitzfaden, C., Zurini, M. G. M., Wider, G., Widmer, H., Wüthrich, K., & Walkinshaw, M. D. (1991) *Nature* 353, 276–279.
- Ke, H. M. (1992) *J. Mol. Biol.* 228, 539–550.
- Ke, H. M., Zydowsky, L. D., Liu, J., & Walsh, C. T. (1991) *Proc. Natl. Acad. Sci. U.S.A.* 88, 9483–9487.
- Ke, H. M., Mayrose, D., & Cao, W. (1993a) *Proc. Natl. Acad. Sci. U.S.A.* 90, 3324–3328.
- Ke, H. M., Zhao, Y., Luo, F., Weissman, I., & Friedman, J. (1993b) *Proc. Natl. Acad. Sci. U.S.A.* 90, 11850–11854.
- Ke, H. M., Mayrose, D., Belshaw, P. I., Alberg, D. G., Schreiber, S. T., Chang, Z. Y., Etzkorn, F. A., Ho, S., & Walsh, C. T. (1994) *Structure* 2, 33–44.
- Kern, D., Kern, G., Scherer, G., Fischer, G., & Drakenberg, T. (1995) *Biochemistry* 34, 13594–13602.
- Kiefhaber, T., Quaas, R., Hahn, U., & Schmid, F. X. (1990) *Biochemistry* 29, 3053–3061.
- Klee, C. B., Draetta, G. F., & Hubbard, M. J. (1988) *Adv. Protein Chem.* 61, 149–199.
- Kofron, J. L., Kuzmic, P., Kichore, V., Colon-Bonilla, E., & Rich, D. H. (1991) *Biochemistry* 30, 6127–6134.
- Lang, K., Schmid, F. X., & Fischer, G. (1987) *Nature* 329, 268–270.
- Liu, J., Albers, M. W., Chen, C. M., Schreiber, S. L., & Walsh, C. T. (1990) *Proc. Natl. Acad. Sci. U.S.A.* 87, 2304–2308.
- Liu, J., Farmer, J. D., Jr., Lane, W. S., Friedman, J., Weissman, I., & Schreiber, S. L. (1991) *Cell* 66, 807–815.
- Mikol, V., Kallen, J., Pflügl, G., & Walkinshaw, M. D. (1993) *J. Mol. Biol.* 234, 1119–1130.
- Mikol, V., Kallen, J., & Walkinshaw, M. D. (1994) *Proc. Natl. Acad. Sci. U.S.A.* 91, 5183–5186.
- Navaza, J. (1994) *Acta Crystallogr.* A50, 157–163.
- Pflügl, G., Kallen, J., Schirmer, T., Jansonius, J. N., Zurini, M. G. M., & Walkinshaw, M. D. (1993) *Nature* 361, 91–94.
- Radzacki, A., Acheson, S. A., & Wolfenden, R. (1992) *Bioorg. Chem.* 20, 382–386.
- Ramachandran, G. N., & Sasisekharan, V. (1968) Conformation of polypeptide and proteins, *Adv. Protein Chem.* 23, 283–437.
- Schönbrunner, E. R., Mayer, S., Tropschug, M., Fischer, G., Takahashi, N., & Schmid, F. X. (1991) *J. Biol. Chem.* 266, 3630–3635.
- Schutkowski, M., Wöllner, S., & Fischer, G. (1995) *Biochemistry* 34, 13016–13026.
- Stein, R. L. (1993) *Adv. Protein Chem.* 44, 1–23.
- Steinmann, B., Bruchner, P., & Superti-Furga, A. (1991) *J. Biol. Chem.* 266, 1299–1303.
- Swanson, S. K. H., Born, T., Zydowsky, L. D., Cho, H., Chang, H. Y., Walsh, C. T., & Rusnak, F. (1992) *Proc. Natl. Acad. Sci. U.S.A.* 89, 3741–3745.
- Takahashi, N., Hayano, T., & Suzuki, M. (1989) *Nature* 337, 473–475.
- Thall, M., Bukovsky, A., Kondo, E., Rosenwirth, B., Walsh, C. T., Sodroski, J., & Göttlinger, H. G. (1994) *Nature* 372, 363–365.
- Thériault, Y., Logan, T. M., Meadows, R., Yu, L., Olejniczak, E. T., Holzman, T. F., Simmer, R. L., & Fesik, S. W. (1993) *Nature* 361, 88–91.
- Wolfenden, R., & Radzacki, A. (1991) *Chemtracts* 2, 52–54.
- Zhao, Y., & Ke, H. (1996) *Biochemistry* 35, 7362–7368.
- Zydowsky, L. D., Etzkorn, F. A., Chang, H. Y., Ferguson, S. B., Stolz, L. A., Ho, S. I., & Walsh, C. T. (1992) *Protein Sci.* 1, 1092–1099.